JOURNAL OF THE KOREAN ASTRONOMICAL SOCIETY
29: 119~136, 1996

STATISTICS OF GRAVITATIONAL LENSING BY A GALAXY IN CLUSTER OR IN FIELD *

YOON, SO-YOON AND PARK, MYEONG-GU
Electronic mail : syyoon,mgp@vega.kyungpook.ac.kr
Department of Astronomy and Atmospheric Sciences, Kyungpook National University, Taegu
(Received July 5, 1996; Accepted October 12, 1996)

ABSTRACT

To examine the effect of neighboring galaxies on the gravitational lensing statistics, we performed numerical simulations of lensing by many galaxies. The models consist of a galaxy in the rich cluster like Coma, or a galaxy surrounded by field galaxies in $\Omega_0 = 1$ universe with $\Omega_{gal} = 0.1$, $\Omega_{gal} = 0.3$ or $\Omega_{gal} = 1.0$, where Ω_{gal} is the total mass in galaxies. Field galaxies either have the same mass or follow Schechter luminosity function and luminosity-velocity relation. Each lensing galaxy is assumed to be singular isothermal sphere (SIS) with finite cutoff radius.

In most simulations, the lensing is mainly due to the single galaxy. But in $\Omega_{gal} = 0.3$ universe, one out of five simulations have 'collective lensing' event in which more than two galaxies collectively produce multiple images. These cases cannot be incorporated into the simple 'standard' lensing statistics calculations. In cases where 'collective lensing' does not occur, distribution of image separation changes from delta function to bimodal distribution due to shear induced by the surrounding galaxies. The amount of spread in the distribution is from a few % up to $\sim$ 50% of the mean image separation in case when the galaxy is in the Coma-like cluster or when the galaxy is in the field with $\Omega_{gal} = 0.1$ or $\Omega_{gal} = 0.3$. The mean of the image separation changes less than 5% compared with a single lens case. Cross section for multiple image lensing turns out to be relatively insensitive to the presence of the neighboring galaxies, changing less than 5% for Coma-like cluster and $\Omega_{gal} = 0.1$, 0.3 universe cases.

So we conclude that Coma-like cluster or field galaxies whose total mass density $\Omega_{gal} < 0.3$ do not significantly affect the probability of multiple image lensing if we exclude the 'collective lensing' cases. However, the distribution of the image separations can be significantly affected especially if the 'collective lensing' cases are included. Therefore, the effects of surrounding galaxies may not be negligible when statistics of lensing is used to deduce the cosmological informations.

Key Words : gravitational lens, galaxy, cluster, cosmology

I. INTRODUCTION

Eddington (1920) was the first who considered the possible existence of multiple images of a source by gravitational lensing. Many theoretical studies have followed since then without any observational evidence for their existence, until the first discovery of multiple imaged lens system, Q0957+561, in 1979 (Walsh, Carswell and Weymann 1979). It has two images of the same QSO and angular separation between the two images is $\sim 6''$. The two images are thought to be the result of lensing by a galaxy aided by the cluster (Young et al. 1981). Since then, more cases of multiple image lens systems have been found. At present there are about ten cases of accepted multiple imaged sources and similar number of candidates (Surdej et al. 1993). Generally the maximum image separations of observed multiply imaged lens systems have larger values than the anticipated separations in the simple lens model.

* This work is in part supported by KOSEF directed research grant 94-1400-04-01-3.

From these gravitational lens systems the mass distribution of the intervening object (i.e. lens) and the property of the spacetime in between can be revealed. To probe the mass distribution of the lens or structure of the source, detailed modelings have been used. To test the cosmological model, gravitational lensing statistics has been employed: the statistical properties of lens systems, such as the probability of multiple imaging and distribution of image separations, have been compared with observations.

This approach became popular after the comprehensive work by Turner, Ostriker and Gott (1984, hearafter TOG). They examined statistical properties of lens systems, with QSOs as sources and galaxies as lenses in the standard Friedmann-Robertson universe, modelling lens galaxies as point masses or isothermal spheres. They calculated analytically the mean angular separation of images, optical depth, i.e., lensing probability, and most probable lens position for each lensing model and compared the expectation with observations.

Gott, Park and Lee (1989) applied these statistical analysis of lensing to diverse cosmological models. They calculated optical depth and expected value for the separation of the images in each cosmological model and especially on the properties of the closed universe model.

Fukugita and Turner (1991, hearafter FT) estimated the frequencies of multiple image galaxy-QSO lensing with more realistic treatment by considering galaxy velocity dispersion distribution based on currently available data, galaxies of non-singular and non-spherical mass distribution, angular resolution selection effects and amplification bias selection effects. Fukugita, Futamase, Kasai and Turner (1992, hereafter FFKT) extended the work including more details and derived the same conclusion that current gravitational lens data exclude the universe dominated by cosmological constant. They also pointed out the uncertainties of physical and statistical formulations at the lensing calculations like ambiguities in the distance formula. However, all these works on statistics of lensing are based on linear analysis treating each gravitational lens as isolated lens system and neglected the effect of surrounding mass distribution such as galaxies.

Recently, to test cosmogonic models Cen et al. (1994) and Wambsganss et al. (1994) investigated gravitational lensing by matter distributed in 3-dimensional (3D) space using ray-shooting methods. They described 3D matter as sum of multiple 2D matter and the matter distributions were taken from simulated cosmic structure formulation in the specific cosmological model. However, due to the limited size of the simulation, their model distribution of matter is too coarse to faithfully represent the individual galaxies. Hence their calculated separation can not be compared reliably with the most of the observations of gravitational lens systems, all of which have separations of images, $\Delta\theta \leq 10''$.

In this paper we perform numerical simulation in order to examine the effect of neighboring mass distribution on the gravitational lensing statistics. We simulate lensing by neighboring mass distribution around a galaxy for several cases and analyze the properties of multiple image systems in particular. We simulate cases with a galaxy in the rich cluster like Coma and a galaxy surrounded by randomly distributed field galaxies under different conditions, such as different cosmological models, cutoff radii, and galaxy masses. We calculate probability distribution of image separation and multiple image cross section as important statistical quantities. Each lensing galaxy is modeled as a singular isothermal sphere (hereafter SIS) whose mass distribution is characterized by one-dimensional velocity dispersion, $v_{\|}$, and image separation is defined to be the maximum separation between any two images in a multiple image system.

In §II description of mass models, lensing equation and the distance foumulae are given. In §III models of neighboring mass distribution are described. In §IV computational method for each model is given. In §V the results of the simulations in terms of probability distribution of image separation and multiple image cross section are presented and discussed. In §VI the effect of neighboring galaxies on gravitational lensing is summarized.

II. FORMULATION OF PROBLEMS

(a) Mass Models

We model discrete lensing matter (galaxies) as truncated SISs, whose projected mass profiles in lens plane are given as (Katz and Paczynski 1987; KP hereafter),

$$M_k(r_k) = \begin{cases} \alpha_k M_G \dfrac{r_k}{R_{c,k}} & \text{for} \quad 0 < r_k < R_{c,k} \\ \alpha_k M_G & \text{for} \quad r_k > R_{c,k}, \end{cases} \tag{1}$$

where k indicates the object number of SIS galaxy, M_G is the fundamental mass of main lensing galaxy and $R_{c,k}$ is the cutoff radius of k-th galaxy. Mass fraction factor α_k is introduced to discriminate the mass of galaxies. The SIS has mass proportional to the one-dimensional velocity dispersion, $v_{\|}$, and radius r_k and is truncated at the cutoff radius $R_{c,k}$. For $r_k > R_{c,k}$, it is same as the point mass. Here, we do not consider the finite size of the core of galaxy.

(b) Lens Equations

Mass distribution in lens plane consists of two components: One is continuous matter, $\Sigma_c(x,y) = \int \rho(x,y,z)dz$, where $\rho(x,y,z)$ is a continuous mass density distribution and another is discrete one Σ_d which is described by the function $M_k(r_k)$. The x- and y-coordinates are chosen to be centered on the deflector's plane and the z-coordinate is aligned with the line of sight of observer. The position of distant source projected into lens plane is (x_0, y_0), the position of discrete matter is (x_k, y_k) and the observed positions of images in the lens plane are (x,y), which satisfy the lens equation (KP),

$$\begin{aligned} (x-x_0) - \frac{4GD}{c^2}\Big[\int\int \Sigma_c(x',y')\frac{x-x'}{r'^2}dx'dy' + \sum_k^N M_k(r_k)\frac{x-x_k}{r_k^2}\Big] = 0, \\ (y-y_0) - \frac{4GD}{c^2}\Big[\int\int \Sigma_c(x',y')\frac{y-y'}{r'^2}dx'dy' + \sum_k^N M_k(r_k)\frac{y-y_k}{r_k^2}\Big] = 0, \end{aligned} \tag{2}$$

where r' and r_k are given as $r'^2 = (x-x')^2 + (y-y')^2$, and $r_k^2 = (x-x_k)^2 + (y-y_k)^2$, and effective distance is defined as $D \equiv D_d D_{ds}/D_s$, where $D_d = d(0,z_d)$, $D_{ds} = d(z_d,z_s)$, and $D_s = d(0,z_s)$ are the angular diameter distances (see, II-c) between the observer and the deflector, between the deflector and the source, and between the observer and the source, respectively. Here, z_d, z_s are the redshifts of the lens and the source and N is the total number of discrete lensing objects under consideration.

Gravitational lens equation, Eq.(2) can be presented in the form of Fermat's principle in optics. Fermat's principle is that light rays from the source traverse to observer along the geodesic of spacetime whose light travel time is minimum (Schneider, Ehlers and Falco 1992). We define Fermat potential, $\phi(x,y)$, which proportional to the light travel time from a source through the point (x,y) in the lens plane to observer. This function, $\phi(x,y)$ contains two effects of time delay: geometrical one due to the difference of path length for different paths and potential one due to passage through gravitational potential. Images of the source appear at the minima, maxima and at the saddle points of Fermat potential i.e., the positions satisfying lens equation $\nabla\phi(x,y) = 0$. These conditions satisfy the Eq (2). In the case of truncated SIS, ϕ is given as (KP)

$$\begin{aligned} \phi(x_0,y_0,x,y) =& \frac{1}{2}(x-x_0)^2 + \frac{1}{2}(y-y_0)^2 - \frac{4GD}{c^2}\Big[\int\int \Sigma_c \ln r' dx'dy' + \sum_k^N \alpha_k M_G \frac{r_k}{R_{c,k}}\Big] \quad \text{for} \quad 0 < r_k < R_{c,k} \\ \phi(x_0,y_0,x,y) =& \frac{1}{2}(x-x_0)^2 + \frac{1}{2}(y-y_0)^2 - \frac{4GD}{c^2}\Big[\int\int \Sigma_c \ln r' dx'dy' + \sum_k^N \alpha_k M_G \ln r_k\Big] \quad \text{for} \quad r_k > R_{c,k} \end{aligned} \tag{3}$$

The dimensionless surface mass density of continuous matter is given as $\sigma_c = \Sigma_c/\Sigma_{crit}$, where the critical surface mass density is defined as $\Sigma_{crit} \equiv c^2/4\pi GD$. Then, the lens equation can be rearranged by the use of dimensionless surface mass density of continuous matter. To make units dimensionless, all parameters are divided by R_0, the Einstein ring radius of a point mass lens with mass M_G, ${R_0}^2 \equiv 4GDM_G/c^2$. We use the same notations for all

dimensionless parameters. The normalized Fermat potential is now,

$$\begin{aligned}\phi(x_0,y_0,x,y) =& \frac{1}{2}(x-x_0)^2+\frac{1}{2}(y-y_0)^2+\frac{1}{2}\sigma_c(x^2+y^2)-\sum_k^N \alpha_k \frac{r_k}{R_{c,k}} \quad \text{for} \quad 0<r_k<R_{c,k},\\ \phi(x_0,y_0,x,y) =& \frac{1}{2}(x-x_0)^2+\frac{1}{2}(y-y_0)^2+\frac{1}{2}\sigma_c(x^2+y^2)-\sum_k^N \alpha_k \ln r_k \quad \text{for} \quad r_k>R_{c,k}\end{aligned} \tag{4}$$

The dimensionless surface mass density for discrete matter is given as

$$\sigma_d = \frac{1}{r^2}\sum_k^N \alpha_k, \tag{5}$$

where r is the dimensionless field range. If all galaxies have the same masses, i.e. $\alpha_k = 1$, then, $\sigma_d = N/r^2$.

For an isolated lens system following truncated SIS mass models, if a source position projected to lens plane is located in the radius R_0^2/R_c, there exist two images. Image separation between the two images is different depending on the cutoff radius. For $R_c > R_0$, image separation is always two times Einstein ring radius, $2r_0$. For $R_c < R_0$, image separation depends on source position relative to the lens position. The Einstein ring radius r_0 is given as

$$r_0 = \begin{cases} R_0 & \text{for} \quad R_c < R_0 \\ \dfrac{R_0^2}{R_c} & \text{for} \quad R_c > R_0 \end{cases} \tag{6}$$

We mainly consider models with galaxies of the cutoff radius, $R_c > R_0$.

When the effect of the surrounding galaxies are ignored, the probability of producing multiple images by a source is equal to the fraction of area covered by the circles of radius R_0^2/R_c of all SIS lenses:

$$\tau_0 = \frac{1}{r^2}\sum_k^N \alpha_k \frac{R_{0,k}^2}{R_{c,k}^2} \tag{7}$$

If all galaxies have the same masses and the same cutoff radii, the probability for multiple image lensing is $\tau_0 = \sigma_d R_0^2/R_c^2$.

(c) Angular Diameter Distance

There can be several definitions of distance in cosmology (Weinberg 1972). It is the angular diameter distance which is relevant in gravitational lensing, because it relates the angular separation to the proper distance.

If the universe is filled with homogeneous and isotropic fluid on the large scales, it satisfies Friedmann-Lemâitre-Robertson-Walker (FLRW) geometry. In this universe, the standard Friedmann-Lemâitre angular diameter distance called as the standard distance can be used (FFKT). This is sometimes referred to as the filled beam case because the light rays are propagated into the space filled with homogeneous and isotropic fluid.

However, gravitational lensing takes place in a clumpy universe. If certain mass fraction $\tilde{\alpha}$ of all matter in the universe is distributed uniformly and the rest is clumped into galaxies, the light rays traverse the space filled with smooth mass having fraction $\tilde{\alpha}$ of all the mass and are affected by the clumpy matter having mass fraction of the rest. The Dyer-Roeder distance takes the effect into consideration (Dyer and Roeder 1973). If $\tilde{\alpha} = 0$, mass distribution is completely clumpy, and if $\tilde{\alpha} = 1$, completely homogeneous. This is called an empty beam case because light rays traverse through vacuum between the clumpy matter.

III. DESCRIPTION OF MODELS

(a) A Galaxy within Rich Cluster

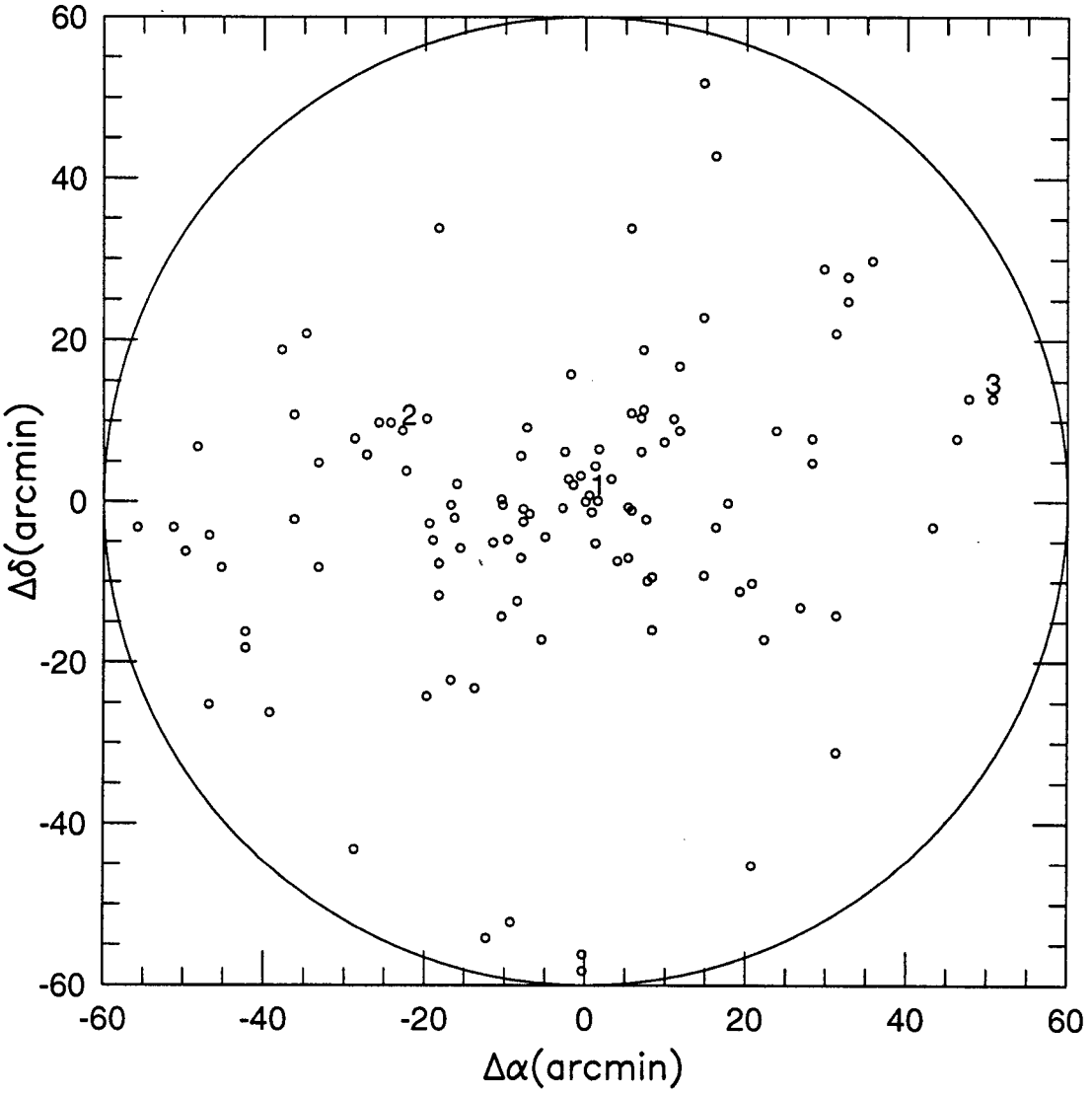

Fig. 1. Spatial distribution of galaxies in radius 1° region from the Coma cluster. The radius of circle is cutoff radius, $R_c = 0.5'$ considered in this model. Each number, 1, 2 and 3 indicates the selected main lensing galaxy.

To study the gravitational lensing by a galaxy within a cluster, we need to have a proper model cluster. We take the Coma cluster as the model cluster.

The position of NGC4874 ($\alpha_{1950} = 12^h57.18^m$, $\delta_{1950} = 28°13'.8$) is adopted as the Coma center. Our simulation is restricted to the region $R \leq 1°$ from the cluster center and galaxies brighter than 15.7 visual magnitude. Galaxies with velocity dispersion between $4000\,\mathrm{km\,s^{-1}} \leq v \leq 10,000\,\mathrm{km\,s^{-1}}$ and with distinct morphological type are included as members of Coma cluster, resulting in 112 galaxies in the cluster. We use the data in Kent and Gunn (1980), the CfA survey by Huchra et al., (1990), and Karachentsev and Kopylov (1990). Figure 1 shows the spatial distribution of galaxies in radius 1° region from the center of Coma cluster.

We fix the cosmological parameters, $\Omega_0 = 1.0$, $\lambda_0 = 0$, and $H_0 = 50\,\mathrm{kms^{-1}Mpc^{-1}}$. To mimic the actual galaxy in gravitational lens system, the model cluster is put at $z_d \simeq 0.421$, at which point the angular diameter for given z_s is the smallest. Source plane is selected at $z_s = 2.0$. All galaxies have the same cutoff radius, $R_{c,k} = R_c = 0.5'$ at $z_d = 0.023$, therefore $R_c = 2.93''$ at $z_d = 0.421$ and the same mass $M_k = M_G$.

Four sets of models are considered. Two of them are the cases having only discrete matter, i.e. galaxies with the mass of $M_G = 10^{11}\,\mathrm{M_\odot}$ or $10^{12}\,\mathrm{M_\odot}$. Putting $M_G = 10^{11}\,\mathrm{M_\odot}$ makes the dimensionless surface mass density of the whole cluster $\sigma_d = 3 \times 10^{-4}$, and $\sigma_d = 3 \times 10^{-3}$ for $M_G = 10^{12}\,\mathrm{M_\odot}$. The other two models include continuous matter,

like smoothly distributed dark matter: continuous matter is 10% of total mass of discrete matter, and galaxies as discrete matter have the mass of $M_G = 10^{11}\,M_\odot$ or $10^{12}\,M_\odot$ in these models. We select a galaxy in three different positions within the cluster as the main lensing galaxy: one near the center, one in the middle of the cluster, and one near the boundary, each designated as 1, 2, and 3 in Figure 1.

(b) A Galaxy Surrounded by Field Galaxies

Next, we simulate the situation when the lensing galaxy is one of the field galaxies. Here we consider only $\Omega_0 = 1.0$, $\lambda_0 = 0$, and $H_0 = 50\,\mathrm{kms}^{-1}\mathrm{Mpc}^{-1}$ flat universe with Ω_{gal} fraction of the mass being in the form of SIS galaxies.

We put main lensing galaxy at the center of the field and distributed 29 galaxies randomly within the field satisfying the given dimensionless surface mass density. For $\Omega_0 = 1.0$ universe, the integrated dimensionless surface mass density between observer and a source at redshift $z_s = 1.5$ is $\sigma \simeq 0.2$ (KP).

We consider two different ways of assigning mass to galaxies:

i) Galaxies of same mass

For this model, we assume all galaxies have the same mass either in $\Omega_{gal} = 1.0$ or $\Omega_{gal} = 0.1$ universe. In $\Omega_{gal} = 1.0$ universe model, since all the masses are in discrete form, the light rays are propagated in the vacuum, and the Dyer-Roeder distance with $\tilde{\alpha} = 0$ is used. Galaxies are placed randomly within the circular field of radius $(30/0.2)^{1/2}R_0 \simeq 12.25R_0$ and have the cutoff radius in unit of R_0, $b \equiv R_{c,k}/R_0 = 2$ whose Einstein ring radius is $r_0/R_0 = R_0/R_c = b^{-1}$. In $\Omega_{gal} = 0.1$ model, we assume that only 10% of the mass in $\Omega_0 = 1.0$ universe reside in galaxies ($\sigma_d = 0.02$). Galaxies are now placed within the circular field of larger radius $(30/0.02)^{1/2}R_0 \simeq 38.73R_0$. Here we consider two sets of models having the cutoff radius $b = 2$ or 5. In this definition, larger b for given Ω_{gal} means galaxies are more extended, i.e., less surface mass density, while the total mass of the individual galaxy is the same. For this case, 20 ensembles are generated for each b.

ii) Galaxies following Schechter luminosity function

To simulate more realistic galaxies, we use Schechter luminosity function of galaxies (Efstathiou, Ellis and Peterson 1988):

$$\phi(L)dL = \phi^*\left(\frac{L}{L^*}\right)^{\alpha} e^{(-L/L^*)} d\left(\frac{L}{L^*}\right), \tag{8}$$

with $\phi^* = (1.56\pm0.4)\times10^{-2}h^3\,\mathrm{Mpc}^{-3}$, $\alpha = -1.1\pm0.1$, and $L^* = 3.68\times10^{10}\,L_\odot$. The empirical relationship between the luminosity and one dimensional velocity dispersion is adopted,

$$\frac{v_{\|}}{v^*} = \left(\frac{L}{L^*}\right)^{a}, \tag{9}$$

where $a = 1/4$ based on Faber-Jackson relation (1976) for ellipticals (E) or lenticulars (SO) and $a = 1/2.6$ based on Tully-Fisher relation (1977) for spirals (S) in the B band. The one component velocity dispersion v^* for a galaxy with the characteristic luminosity is also estimated to be (FT)

$$v^* = \begin{cases} 276^{+15}_{-24} & \mathrm{kms}^{-1} \quad \text{for} \quad E \\ 252^{+15}_{-24} & \mathrm{kms}^{-1} \quad \text{for} \quad SO \\ 144^{+8}_{-13} & \mathrm{kms}^{-1} \quad \text{for} \quad S \end{cases} \tag{10}$$

And the morphological composition of galaxies are $E : SO : S = 12\pm2 : 19\pm4 : 69\pm4$ (FT).

Since the mass of SIS galaxy is

$$M_k = \frac{2v_{\|}^2}{G}R_{c,k}, \tag{11}$$

we need to determine the cutoff radius $R_{c,k}$ in addition to the velocity dispersion which is randomly generated according to the luminosity function. But there is hardly anything known about the size of the isothermal halo of

Table 1. Multiple image lensing by a galaxy in a cluster

	$M_G^{2)}/M_\odot$	$\sigma_d^{3)}$	$\sigma_c^{4)}$	range of $\Delta\theta/r_0^{5)}$	$<\Delta\theta/r_0>^{6)}$	$\text{STDEV}^{7)}_{\Delta\theta/r_0}$	$\text{X}^{8)}$
case 1[1)]	10^{11}	3×10^{-4}	0.0	$1.987\sim2.014$	2.000	0.009	0.97
(center)	10^{12}	3×10^{-3}	0.0	$1.835\sim2.172$	2.014	0.094	0.97
	10^{11}	3×10^{-4}	3×10^{-5}	$1.987\sim2.014$	2.000	0.009	0.97
	10^{12}	3×10^{-3}	3×10^{-4}	$1.837\sim2.173$	2.014	0.094	0.97
case 2[1)]	10^{11}	3×10^{-4}	0.0	$1.991\sim2.009$	2.000	0.006	1.02
(intermediate)	10^{12}	3×10^{-3}	0.0	$1.867\sim2.105$	2.004	0.067	1.01
	10^{11}	3×10^{-4}	3×10^{-5}	$1.991\sim2.009$	2.000	0.006	1.03
	10^{12}	3×10^{-3}	3×10^{-4}	$1.856\sim2.106$	2.006	0.067	1.02
case 3[1)]	10^{11}	3×10^{-4}	0.0	$1.997\sim2.003$	2.000	0.002	0.96
(outer)	10^{12}	3×10^{-3}	0.0	$1.968\sim2.031$	2.000	0.021	0.94
	10^{11}	3×10^{-4}	3×10^{-5}	$1.997\sim2.003$	2.000	0.002	1.00
	10^{12}	3×10^{-3}	3×10^{-4}	$1.969\sim2.031$	2.001	0.021	0.95

1) Case 1 is when the main lensing galaxy is located at the center of the cluster, case 2 at the intermediate, and case 3 at the outer part. 2) Mass of an individual galaxy. 3) The dimensionless surface mass density of whole cluster in discrete matter, i.e., galaxies. 4) The dimensionless surface mass density of whole cluster in continuous matter. 5) Range of image separation, $\Delta\theta/r_0$ (the minimum and the maximum value). 6) The mean of $\Delta\theta/r_0$. 7) The standard deviation of $\Delta\theta/r_0$. 8) The cross section for multiple image lensing by a galaxy within the cluster in unit of that by a single galaxy, calculated from the simulation.

galaxies, and therefore we arbitrarily set $R_{c,k} = bR_{0,k}$ where b is constant. Then, cutoff radius $R_{c,k}$ is determined self-consistently in the Eq (11). This assures that the lensing occurs within the isothermal part of model galaxies.

In one ensemble we generate 30 random galaxies within the interval $10^{-4}L^* \sim 5L^*$ to get $v_{||}$ and $R_{c,k}$ using above relations. They are placed in $z_d \simeq 0.37$ lens plane for $z_s = 1.5$ source to see the maximum gravitational lensing effect. The luminosity of main lensing galaxy L_G is set to L^*.

Integrate the Schechter luminosity function using the constant mass to light ratio model (van der Marel, 1991),

$$\left(\frac{M}{L}\right)_B = \left(\frac{M}{L}\right)_{B^*}\left(\frac{L}{L^*}\right)^\beta \tag{12}$$

where $(M/L)_{B^*} = (10\pm2)h$ and $\beta = 0.25\pm0.10$ gives $\Omega_{gal} \sim 0.3$. We don't expect real Ω_{gal} to be larger than 0.3, because even when we assume galaxies constitute 100% of the cluster mass, we get $\Omega \lesssim 0.3$. So we consider $\Omega_{gal} = 0.1$ and $\Omega_{gal} = 0.3$ cases. For each $b = 2$ and $b = 5$, 20 ensembles are generated in $\Omega_{gal} = 0.1$ and 30 ensembles in $\Omega_{gal} = 0.3$.

IV. CALCULATIONS

We place 2401 source points within the square of length $8r_0$ centered on main lensing galaxy and 112 of them are within the Einstein ring of the main lensing galaxy of radius r_0. For each source position, the lens equation (Eq. 4) is solved by Newton-Rhapson method for nonlinear systems of equations (Press et al., 1986), and the image position for each source is found. We select the source positions producing multiple images and calculate the maximum separation, $\Delta\theta$, among the multiple images of the same source. The probability distribution of maximum image separations are calculated from $\Delta\theta$'s. Cross section for the multiple imaging is calculated by counting the number of the sources which produce multiple images and divide by the number of sources within the Einstein circle of the main lensing galaxy. When source positions producing multiple images are not contained within the 2401 source positions, we increase the number of source positions toward the displaced direction and recalculate.

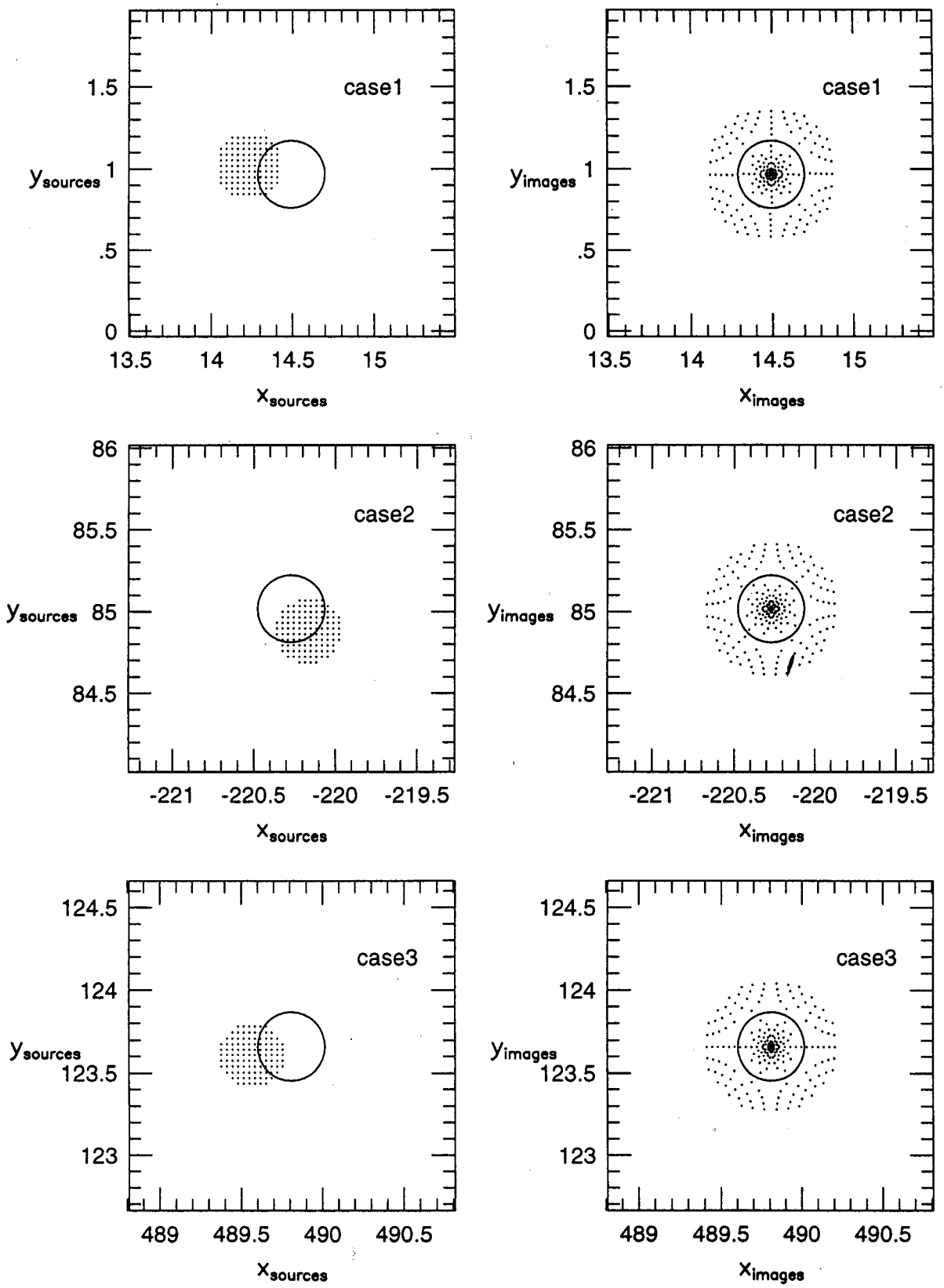

Fig. 2. Typical source positions (left panel) producing multiple images and image positions (right panel) for $\sigma_d = 3 \times 10^{-4}$ cluster ($M_G = 10^{11}\, M_\odot$): Case 1 is for a galaxy at the center, case 2 at the intermediate and case 3 at the boundary of the cluster. The circle is the Einstein ring with radius r_0 and axes are in unit of R_0.

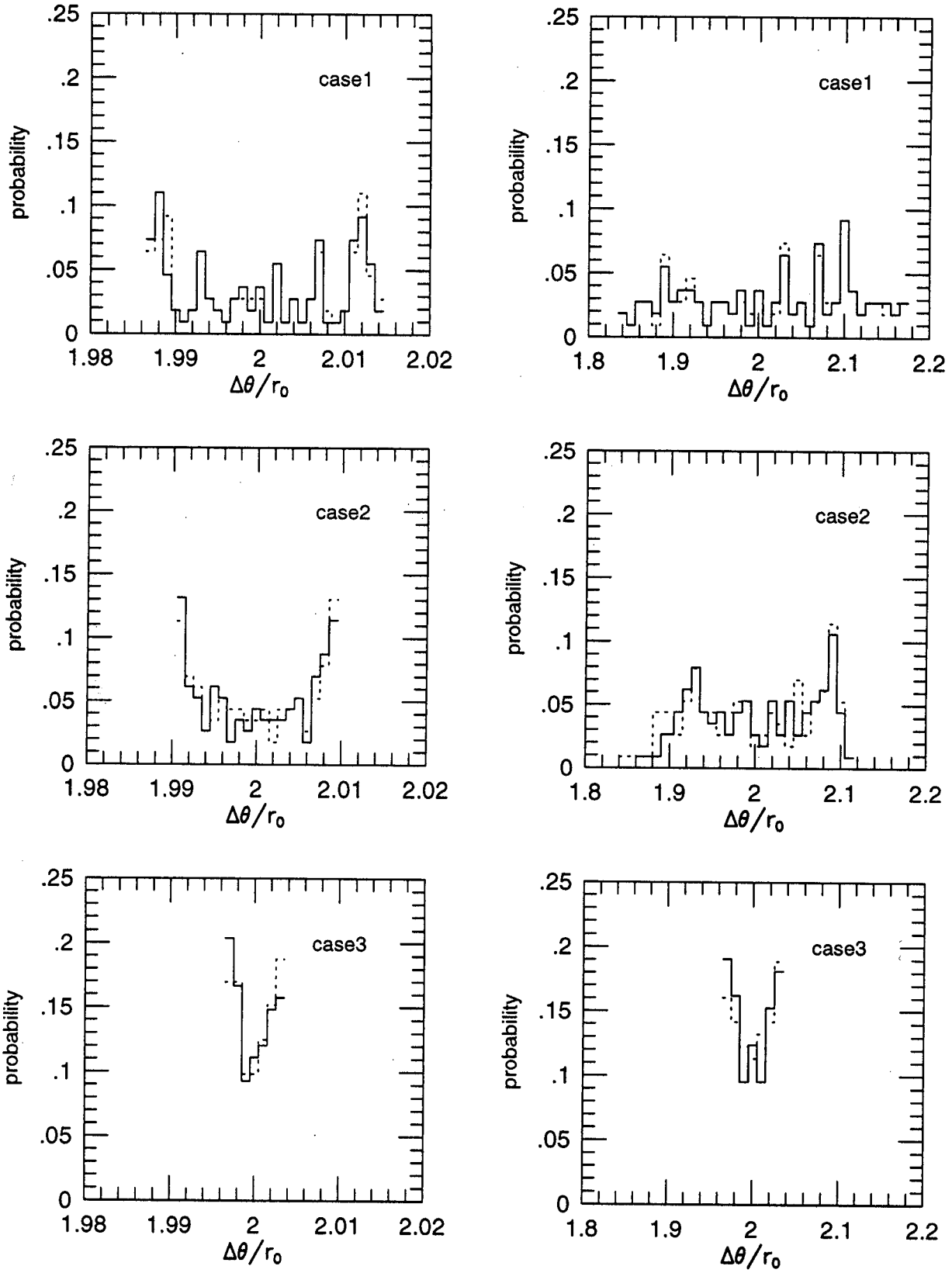

Fig. 3. Relative probability distributions of image separation of Coma cluster models. The dotted line is for the case when continuous matter is included. Left panel is for $\sigma_d = 3 \times 10^{-4}$ cluster ($M_G = 10^{11} M_\odot$), and right for $\sigma_d = 3 \times 10^{-3}$ cluster ($M_G = 10^{12} M_\odot$).

V. RESULTS AND DISCUSSIONS

(a) A Galaxy within Rich Cluster

The mass of individual galaxy, dimensionless surface mass density of whole cluster in continuous and discrete matter (galaxies), the range, the mean and the standard deviation of image separations $\Delta\theta/r_0$, and multiple image lensing cross section are summarized in Table 1 for lensing by a galaxy in Coma-like cluster.

Figure 2 shows the source (left panel) and image (right panel) positions of multiply imaged sources for $\sigma_d = 3\times10^{-4}$ ($10^{11}\,M_\odot$) cluster. Locations of sources producing multiple images are shifted from the Einstein circle, yet their number, hence the cross section for multiple image lensing, is not significantly affected by the cluster galaxies (also see Table 1).

The relative probability distributions of image separations are shown in Figure 3. Left panel is for $\sigma_d = 3\times10^{-4}$ and right for $\sigma_d = 3\times10^{-3}$. The dotted line is when there exists continuous matter in addition. We find that in general the probability distribution of image separation tends to be bimodal. Shear due to the neighboring galaxies make the separations either larger or smaller. There are no significant differences between the case for discrete matter only and the case for discrete and continuous matter distribution, mainly because the surface mass density of continuous matter is only 10% of the total mass.

The image separations are distributed within $(2\pm0.02)r_0$ for $\sigma_d = 3\times10^{-4}$ cluster in contrast to exact $2r_0$ for a single galaxy. The mean and the standard deviation of the image separation is $(2.000\pm0.009)r_0$ when the main lensing galaxy is at the center of the cluster, $(2.000\pm0.006)r_0$ at the intermediate and $(2.000\pm0.002)r_0$ at the outer boundary. So the cluster of this surface mass density can widen the image separation only up to $0.02r_0$: more for the galaxy at the center and less for galaxy at the outer part. For more massive $\sigma_d = 3\times10^{-3}$ cluster, the image separations can decrease or increase up to $0.2r_0$. However the mean of the image separation is increased by only $0.014r_0$.

Multiple image lensing cross sections of the main lensing galaxy also become either smaller or larger up to 4% for $\sigma_d = 3\times10^{-4}$ cluster and 6% for $\sigma_d = 3\times10^{-3}$ cluster, compared with the single SIS lens case (see Table 1). Unlike the image separation, the amount of change in lensing cross section is not correlated with the position within the cluster: intermediate position has largest cross section.

We also tried $\sigma_d \simeq 3\times10^{-2}$ cluster model ($M_G = 10^{13}\,M_\odot$), and in most simulations the effects of neighboring galaxies are too strong to treat their effects individually: we can not say a single galaxy is dominant for lensing. The non-linearity of lensing is too great, and lensing by individual galaxies cannot be added up to estimate lensing by all galaxies which is generally done in standard statistics of lensing calculations. However, we think this choice of cluster mass is probably unrealistic, and will not discuss further.

(b) A Galaxy Surrounded by Field Galaxies

Among many simulations of this kind, we find several cases where two or more galaxies collectively produce multiple images, and the effect of neighboring galaxy cannot be reduced to the perturbation on the single galaxy lensing. In these cases, its effect on statistics of lensing cannot incorporated into the standard lensing statistic calculations in which only one galaxy at a time is assumed to be responsible for lensing. For example, if multiple lensing occurs due to two galaxies with different mass (i.e., velocity dispersions), the image separation or cross section for multiple imaging cannot be parameterized in terms of the velocity dispersion of either galaxy. Also, in real observed lens systems, if more than one galaxies are seen closeby and suspected to be responsible for lensing, these cases are generally excluded when compared with lensing statistics calculations. For these reasons, we define the criterion for these 'collective lensing' cases and exclude them in calculating statistical properties.

These 'collective lensing' cases occur only when two or more galaxies are quite nearby and their masses are comparable. When one galaxy is quite heavier than the other, in terms of the whole statistics of lensing only lensing by the heavier one is important, which is not affected by the nearby presence of the lighter one. So we set two criteria: one for the distance and the other for the mass ratio. First, the distance between the centers of the main lensing galaxy and the nearby one should be less than $2(r_{0,m}+r_{0,n})$, where $r_{0,m}$ and $r_{0,n}$ are the Einstein ring radii of the main and nearby galaxies, respectively. Second, $r_{0,m}/r_{0,n}$ should be less than $\sqrt{10}$: If the ratio $r_{0,m}/r_{0,n} > \sqrt{10}$, then we expect the multiple image lensing cross section by the main galaxy is more than 100 times larger than that

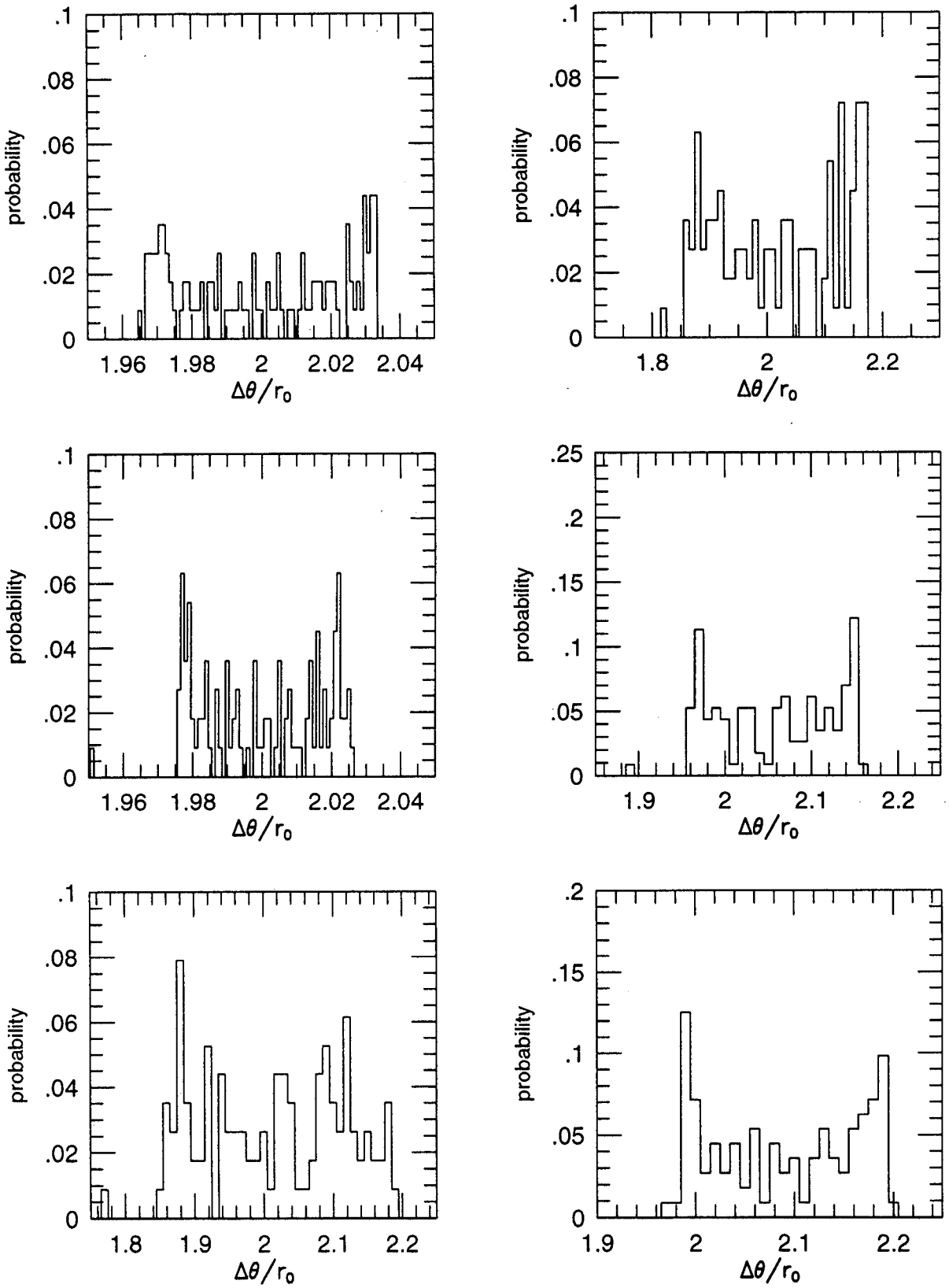

Fig. 4. Some examples of probability distributions of image separation in equal mass field galaxy cases: left panel for $b \equiv R_c/R_0 = 2$ and right panel for $b = 5$ in $\Omega_{gal} = 0.1$ universe.

Table 2. Effect of neighboring field galaxies on gravitational lensing

Model	Case	range of $\Delta\theta/r_0^{1)}$	$<\Delta\theta/r_0>^{2)}$	$\text{STDEV}^{3)}_{\Delta\theta/r_0}$	$<X>^{4)}$	$\text{STDEV}^{5)}_{X}$	$P^{6)}$
$\Omega_{gal}=0.1$	$b=2$	$1.754\sim2.306$	2.005	0.011	0.999	0.019	5%(1/20)
same mass	$b=5$	$1.816\sim2.291$	2.044	0.055	0.996	0.015	0%(0/20)
$\Omega_{gal}=0.1$	$b=2$	$1.713\sim2.823$	2.027	0.092	1.001	0.017	0%(0/20)
SLF[7)]	$b=5$	$1.796\sim2.491$	2.026	0.059	0.998	0.018	5%(1/20)
$\Omega_{gal}=0.3$	$b=2$	$1.750\sim3.093$	2.048	0.133	1.000	0.016	20%(6/30)
SLF[7)]	$b=5$	$1.761\sim2.768$	2.099	0.100	0.999	0.016	3%(1/30)

1) The range of distribution of image separation $\Delta\theta/r_0$. 2) The mean of $\Delta\theta/r_0$. 3) The standard deviation of $\Delta\theta/r_0$. 4) The mean of cross section for multiple image lensing in unit of that in a single galaxy case. 5) The standard deviation of lensing cross section. 6) The probability of 'collective lensing'. 7) Galaxies follow Schechter luminosity function.

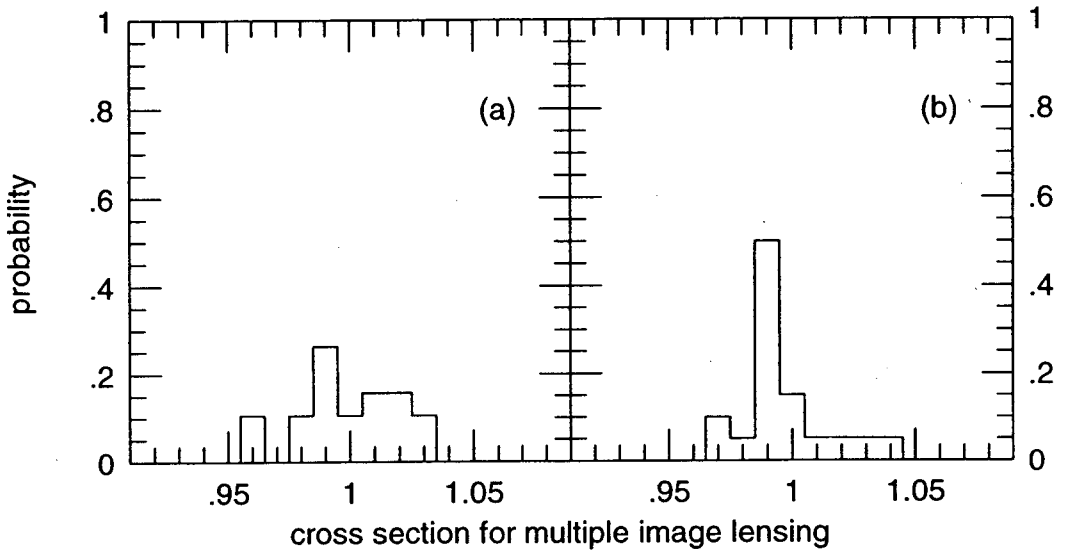

Fig. 5. Relative probability distribution of multiple image lensing cross sections in units of that in a single lens case (a) for $b=2$ and (b) for $b=5$ in $\Omega_{gal}=0.1$ universe.

by the nearby galaxy, and the perturbation of order unity in the cross section by the nearby galaxy could be ignored within 1% level.

(i) Galaxies of the same mass

The $\Omega_{gal}=0.1$ model shows similar probability distribution of image separation as cluster case. The probability distributions of image separation in three simulations ($b\equiv R_c/R_0=2$) are shown in the left panel of Figure 4. Image separations are distributed in the range from $(2\pm0.02)r_0$ to $(2\pm0.2)r_0$, corresponding to $1\%\sim10\%$ deviation from a single galaxy lensing. The range, mean, and standard deviations of $\Delta\theta/r_0$ of all multiple images in 19 simulations except one 'collective lensing' case are listed in Table 2.

The right panel of Figure 4 shows the distribution in $b=5$ simulations. The separations are distributed in the similar range. However, distribution of image separations, on average, is more affected in $b=5$ case than in $b=2$ case. This probably is due to the fact that larger b means galaxies are less compact for a given galaxy mass, resulting in smaller Einstein radius r_0. If the shear due to the surrounding galaxies is mainly determined by Ω_{gal}, then the distribution of the dimensionless quantity $\Delta\theta/r_0$ will be more affected when r_0 is smaller. So we expect more change

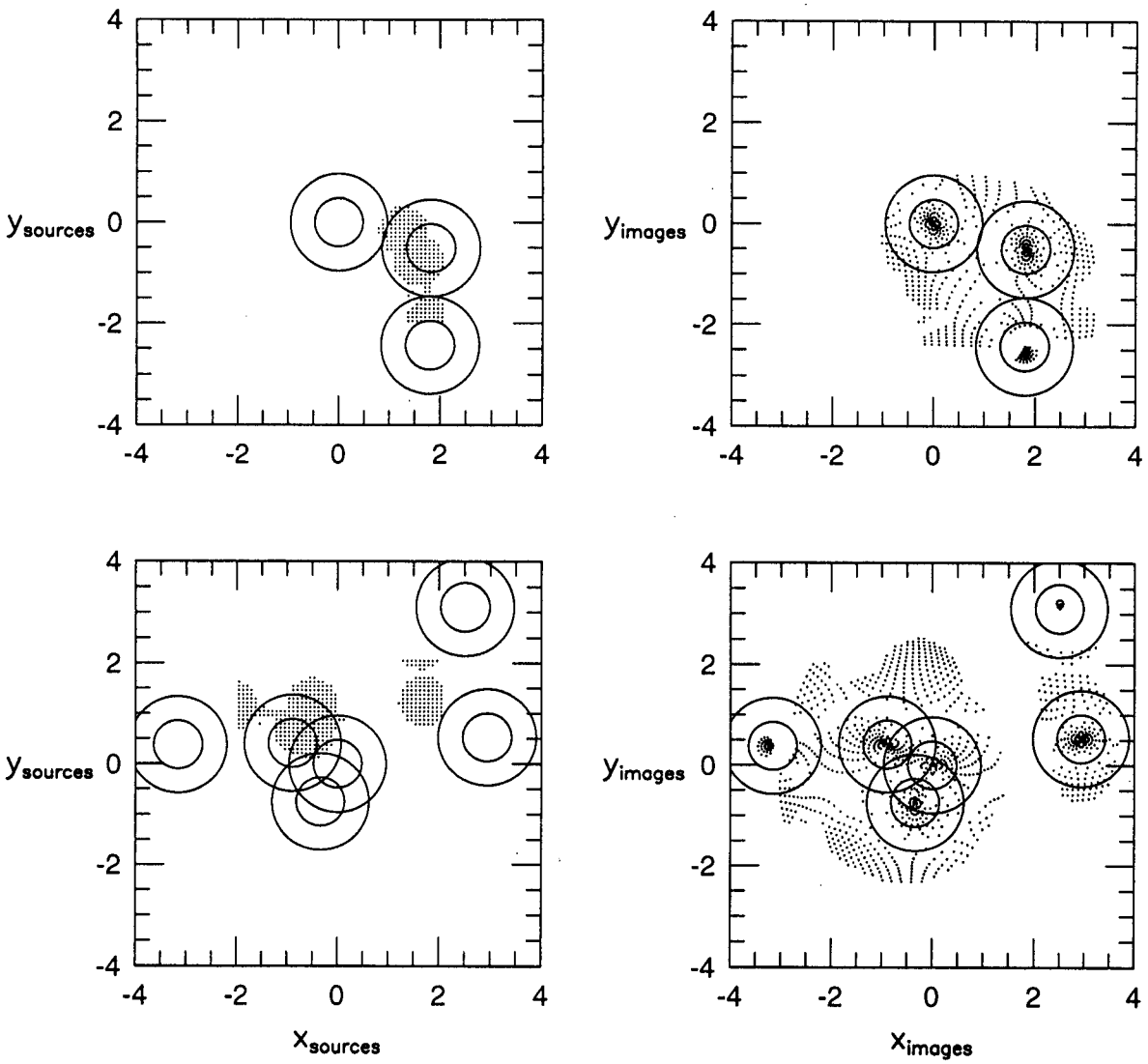

Fig. 6. Examples of 'collective lensing' in $\Omega_{gal} = 1.0$ model: source positions producing multiple images and their corresponding image positions are shown in left and right panels, respectively. The inner circle has radius r_0 and outer circle R_0.

in $\Delta\theta/r_0$ distribution in larger b models.

We also note that the mean of $\Delta\theta$ in all simulations with $b = 5$ is $\sim 0.04r_0$ larger than single lens case. In a few cases, the shift of the $\Delta\theta/r_0$ distribution is quite significant, $\sim 0.1r_0$ (Fig. 4).

The cross section for multiple image lensing is distributed within 5% of single lens case (Fig. 5). Although $b = 5$ case (Fig. 5b) has more centrally peaked distribution than $b = 2$ case (Fig. 5a), we are not sure if this is statistically significant.

We also find that the center of bimodal probability distribution of image separation is shifted to the larger value in half of the $b = 5$ simulations. The shifted amount of the center ranges from $0.02r_0$ to $0.2r_0$. The mean of $\Delta\theta/r_0$ shows this trends well (Table 2). But this shift is less than one standard deviation.

If $\Omega_{gal} = 1.0$, field galaxies have dominant effects on the single galaxy lensing, and 5 out of 10 lensing simulations are found to be 'collective'. Figure 6 shows some examples of $\Omega_{gal} = 1.0$ model. It is not quite meaningful to use the standard lensing statistics calculations in these situations, and we do not derive any statistics from these simulations.

ii) Galaxies following Schechter luminosity function

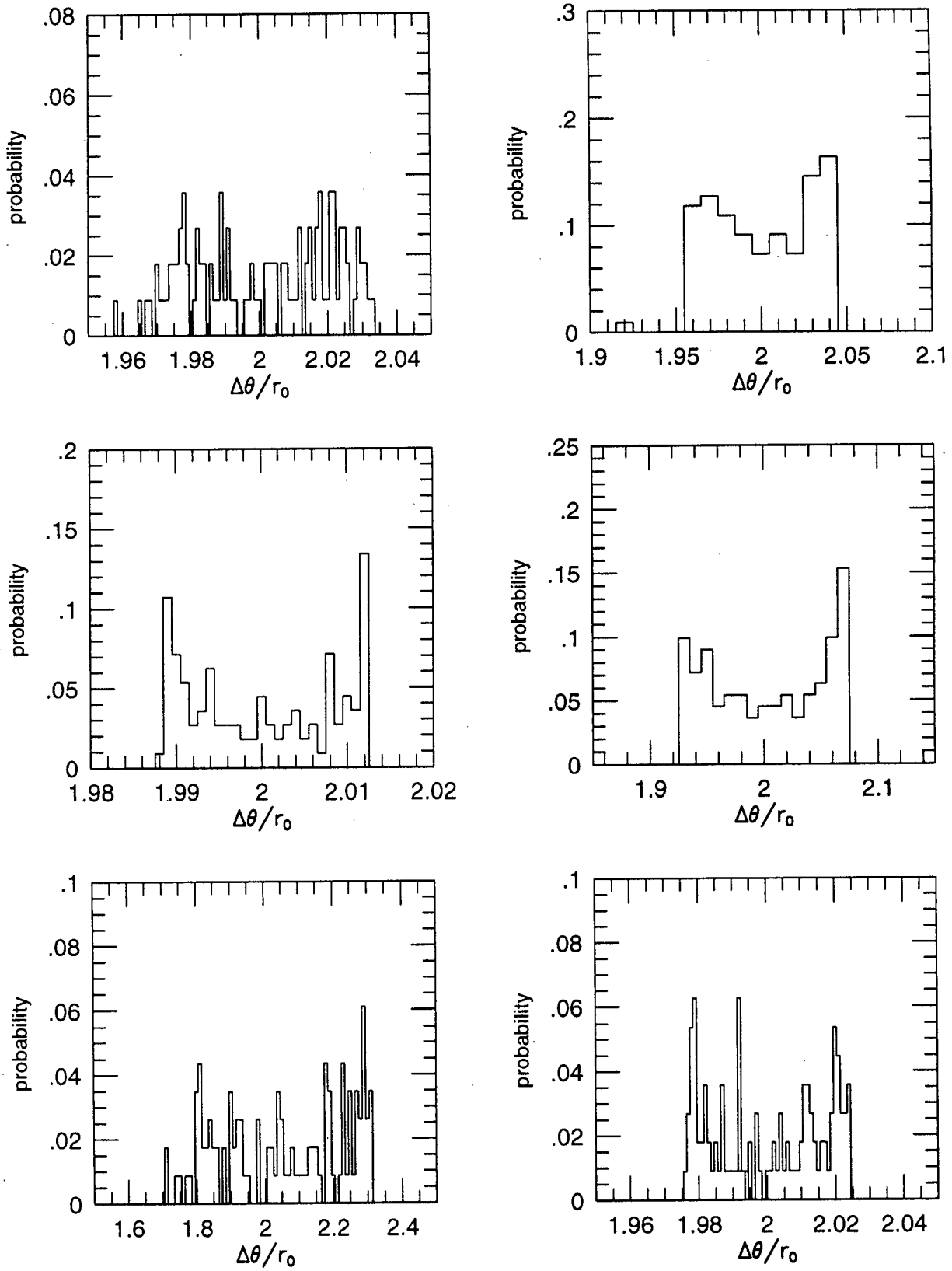

Fig. 7. Some examples of probability distributions of image separations by the galaxy surrounded by field galaxies following Schechter luminosity functions in $\Omega_{gal} = 0.1$ universe: left panel for $b = 2$ and right panel for $b = 5$.

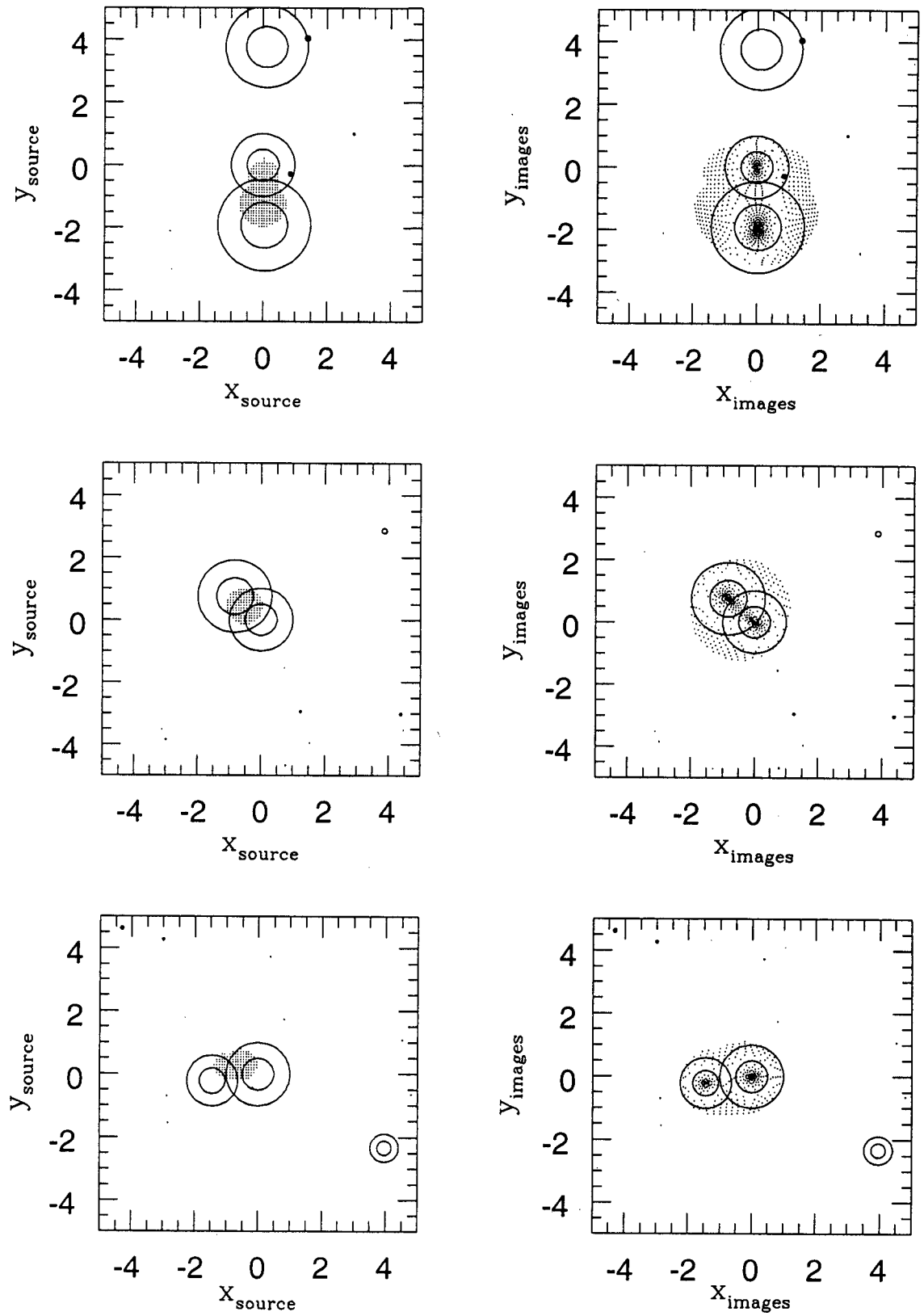

Fig. 8. Some examples of 'collective lensing' by field galaxies ($b = 2$) in $\Omega_{gal} = 0.3$ universe. The inner circle has radius r_0 and outer one R_0. Dots away from the center galaxy are R_0 and r_0 circles for galaxies much fainter than L^*. (see text for details)

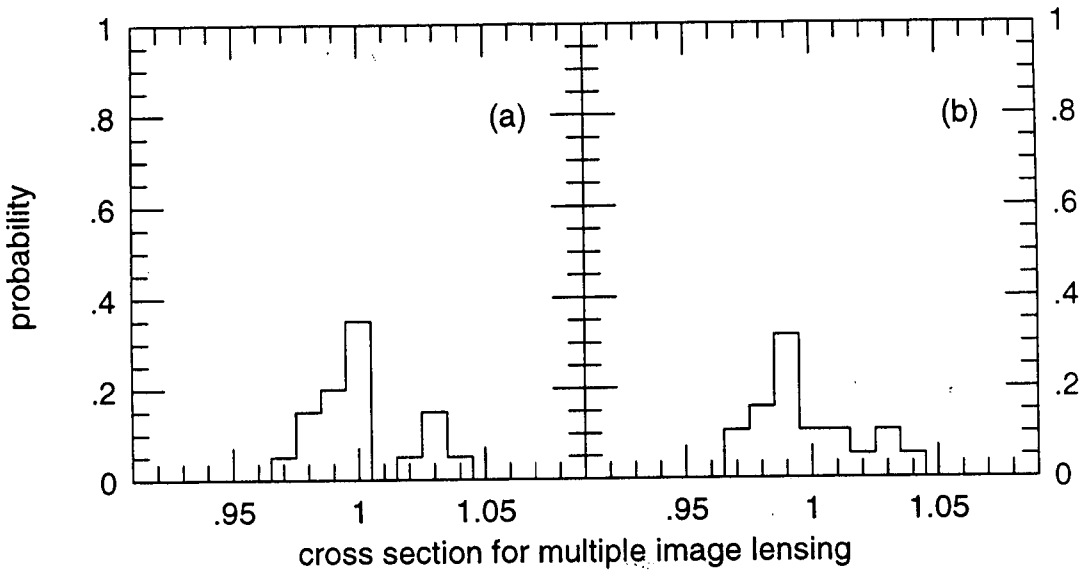

Fig. 9. Probability distribution of multiple image lensing cross sections in units of that in a single lens case. Field galaxies follow Schechter luminosity function in $\Omega_{gal} = 0.1$ universe: (a) for $b = 2$ and (b) for $b = 5$.

In the $\Omega_{gal} = 0.1$ or $\Omega_{gal} = 0.3$ universe with galaxies following Schechter luminosity function, neighboring galaxies have different velocity dispersion, mass, and cutoff radii. Most of the galaxies are smaller in mass than the main lensing galaxy, assumed to be L^* galaxy. The mass, cutoff radius and Einstein ring radius of main lensing galaxy are determined from this model according to the morphological types. The image separation $\Delta\theta$ is constant because the velocity dispersion of the main lensing galaxy is fixed.

Some examples of probability distribution of image separation with $\Omega_{gal} = 0.1$ show again bimodal distribution as shown in the left panel for $b = 2$ and in the right panel for $b = 5$ of Figure 7. We find that the distribution of image separation is widened by $0.5\% \sim 10\%$ for both sets of models, $b = 2$ and 5. Unlike the previous case where galaxies having the same mass, here we pick the velocity of dispersion of galaxies, and r_0, hence image separation and lensing cross section of a single galaxy, does not depend on b. Different b means different galaxy size with same surface mass density. The mean distance between the galaxies are adjusted accordingly since Ω_{gal} is fixed. Larger b means bigger and more massive galaxies separated further away.

In the $\Omega_{gal} = 0.3$ universe, we found 6 out of 30 simulations show 'collective lensing' events in $b = 2$ model(Table 2). Some examples are shown in Figure 8. The inner circle is the Einstein ring of radius r_0 which is the measure of the image separation and of the lensing cross section of each galaxy. The outer circle has radius R_0 which is proportional to the total mass of each galaxy and shows how much mass is distributed in the field (ref. §II). Very small circles, or dots, away from the central galaxies are the Einstein circles for galaxies much fainter than L^*, hence lower velocity dispersion and surface mass density. For these 'collective lensing' cases, we repeat the simulations with only the dominant galaxies at the center and find essentially the same result. So in most cases a single $\sim L^*$ galaxy nearby causes 'collective lensing' event. The simulations that do not show 'collective lensing' event suggest some difference between $b = 2$ and $b = 5$ models (see Table 2): $b = 5$ models have higher mean of $\Delta\theta/r_0$. This difference could be due to the clumpiness of the surrounding matter distribution: larger b means more clumpy mass distribution and therefore larger fluctuation in shear.

Almost all ensembles except 'collective lensing' cases show the bimodal probability distribution of image separations. The distribution of image separation is widened by $0.5\% \sim 50\%$ for $b = 2$ and $2.5\% \sim 40\%$ for $b = 5$ (Table 2). So we do expect to see a small fraction of cases in which the image separation is significantly higher than the single lensing case, even when a massive galaxy is not quite nearby. Also, the mean of the image separation can be as large as $\sim 2.1 r_0$ compared to that in the single lens case, $2r_0$.

However, the change of the cross section for the multiple image lensing by main lensing galaxy is less than 5% both in $\Omega_{gal} = 0.1$ and $\Omega_{gal} = 0.3$ simulations (Fig. 9 and Fig. 10). Since the error due to the finite number of

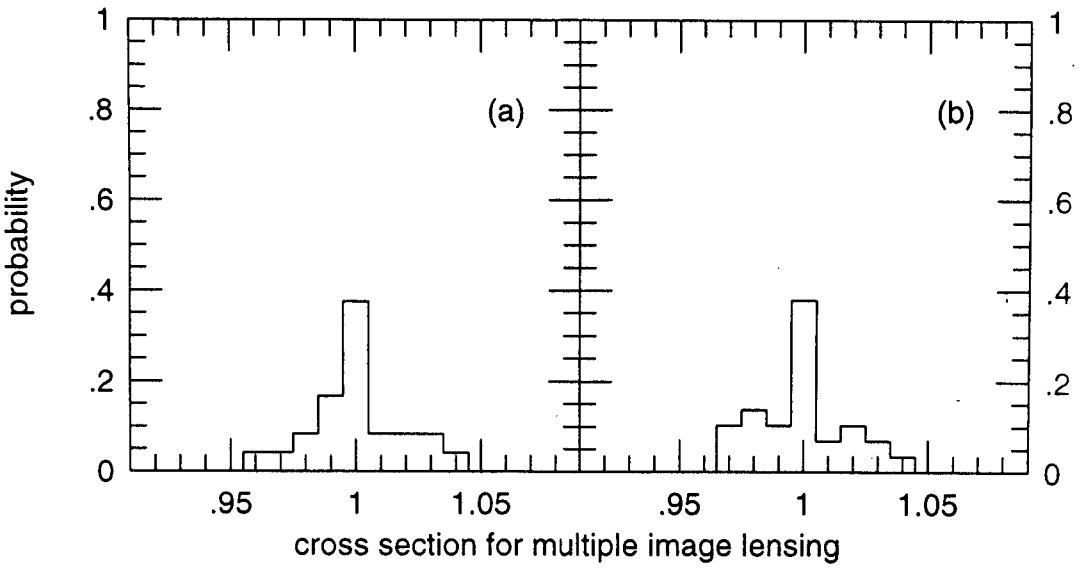

Fig. 10. Same as Figure 9 for $\Omega_{gal} = 0.3$ universe.

source positions in estimating the cross section is on the order of few %, this change is not significant.

VI. SUMMARY

We have simulated gravitational lensing by galaxies in cluster or in fields in order to examine the effects of surrounding galaxies on the gravitational lensing statistics.

We find that in general the image separations are found to follow bimodal distribution due to the shear as opposed to the single value expected in the isolated SIS lens system. The expected image separation is more likely to be slightly smaller or larger than that by a single SIS.

In Coma-like cluster cases, each simulation shows various width in the distribution of image separation, ranging 0.5% to 10% of mean image separation. The width is roughly proportional to the mean surface mass density.

When a lensing galaxy is surrounded by randomly distributed field galaxies which follow the Schechter luminosity function and usual luminosity-velocity relations, we find that most lensing occurs by a single galaxy in $\Omega_{gal} = 0.1$ universe. However, in $\Omega_{gal} = 0.3$ universe with small galaxy cutoff radii one out of five cases is found to contain 'collective lensing' event where more than two galaxies collectively produce multiple images. These cases will produce significantly different image separations and multiple image cross sections than in a single lens case and are difficult to be incorporated into the 'standard' lensing statistics calculations.

Even in cases where 'collective lensing' does not occur, we find that the distribution of image separation is again bimodal and spread quite significant: It can be as large as 40% in $\Omega_{gal} = 0.1$ model and 50% in $\Omega_{gal} = 0.3$ model. However, the mean of the image separations in all simulations together is only $\sim 5\%$ larger than the single galaxy lensing, and the standard deviation $\sim 5\%$ of the image separation. The cross section for multiple image lensing by the main lensing galaxy is found to be less prone to the effect of surrounding galaxies, less than 5% even in $\Omega_{gal} = 0.3$ simulations.

We also simulate somewhat extreme cases: In models with the dominant shear by surrounding galaxies, like in the Coma-like cluster model with $\sigma_d \simeq 3 \times 10^{-2}$ or $\Omega_{gal} = 1.0$ universe model, we find that many images having anomalously large separations can be produced. The effect of surrounding galaxies are not perturbations anymore, and it is necessary to consider lensing by the whole galaxies in the field. Simple sum of lensing by individual galaxies will produce significant errors. The cross section for multiple image lensing also shows significant variations.

We conclude that when a main lensing galaxy is located in the Coma-like cluster or in the field galaxies their total mass being reasonable fraction of that of the universe, the probability of multiple image lensing is not significantly affected especially if the 'collective lensing' cases are excluded. But the image separation distribution can be

significantly changed even when 'collective lensing' does not occur, and the occurrence of 'collective lensing' events cannot be ignored. So we believe the effect of surrounding galaxies is important in gravitational lensing statistics and should be considered when lensing statistics calculation is compared with the observed lens systems to derive various cosmological informations. We will explore the quantitative effects of 'collective lensing' in future work with larger number of simulations.

We thank the Computer Center of Kyungpook National University for generously providing the computing time.

REFERENCES

Cen, R., Gott III, R., Ostriker, J.P. and Turner, E.L., 1994, ApJ, 423, 1
Dyer, C.C. and Roeder, R.C., 1973, ApJ, 180, L31
Eddington, A.S. 1920, Space, time and gravitation, Cambridge University Press, Cambridge
Efstathiou, G., Ellis, R.S., and Peterson, B.A., 1988, MNRAS, 232, 431
Faber, S.M. and Jackson, R.E., 1976, ApJ, 204, 668
Fukugita, M. and Turner, E.L., 1991, MNRAS, 253, 99 (FT)
Fukugita, M., Futamase, T., Kasai, M. and Turner, E.L., 1992, ApJ, 393, 3 (FFKT)
Gott III, J.R., Park, M.-G., Lee, H.M., 1989, ApJ, 338, 1
Huchra, J.P., Geller, M.J., de Lapparent, V. and Corwin, JR., H.G., 1990, ApJS, 72, 433
Karachentsev, I.D. and Kopylov, A.I., 1990, MNRAS, 243, 390
Katz, N. and Paczynski, B., 1987, ApJ, 313, 11
Kent, S.M. and Gunn, J.E., 1982, ApJ, 87, 945 (KG)
Press, W.H., Flannery, B.P., Teukolsky, S.A. and Vettering, W.T., Numerical Recipies, Cambridge University Press, 1986, p269
Schneider, D.P., Ehlers, J., and Falco, E.E., 1992, Gravitatioal Lenses, Springer, Berlin
Surdej, D., Fraipont, D., Gosset, E., and Remy, M., 'Gravitational Lenses in the Universe', Proceedings of the 1993 Leige International Astrophysical Colloquium, 1993
Tully, R.B., and Fisher, J.R., 1977, A&AS, 204, 668
Turner, E.L., Ostriker, J.P. and Gott III, R., 1984, ApJ, 284, 1 (TOG)
van der Marel R.P., 1991, MNRAS, 253, 710
Walsh, D., Carswell, R.F., and Weymann, R.J., 1979, Nature, 279, 381
Wambsganss, J., Cen, R., Ostriker, J.P., and Turner, E.L., 1995, Science, 268, 274
Weinberg, S., 1972, Gravitation and Cosmology, New York Willey
Young, P., Gunn, J.E., Kristian, J., Oke, J.B. and Westphal, J.A., 1981, ApJ., 244, 736